

# Tearing of thin polyimide films

J. A. HINKLEY, C. A. HOOGSTRATEN

*Polymeric Materials Branch, NASA Langley Research Center, Hampton, Virginia 23665-5225, USA*

Films of BTDA-ODA polyimide up to 58  $\mu\text{m}$  thick were torn at constant cross-head speed in "trousers" tests. In common with previous results on polyolefins, the work of tearing was found to increase markedly with specimen thickness. A model for the increase, based on the volume of plastically deformed material adjacent to the crack plane, was found to be only qualitatively valid. The experimental slope of a plot of tearing energy (per unit area) against thickness was  $70 \text{ MJ m}^{-3}$ . Optical and scanning electron micrographs of torn films are discussed in regard to the modes of failure.

## 1. Introduction

The fracture behaviour of polyimides has received very little attention, perhaps because it is usually impractical to prepare specimens in any form other than thin films. These films are generally characterized by simple tensile tests (e.g. [1]) although impact and Elmendorf tear values were reported by Wallach [2]. Theocaris *et al.* [3] used notched tensile specimens to study the effect of increasing imidization on ductility and mode I stress intensity factor.

Efforts to improve the toughness of polyimide films (e.g. [4]) called for the development of simple, meaningful test methods for tear resistance, and the ASTM single tear method [5] has been shown to be appropriate. This "trousers" test was originally applied by Rivlin and Thomas [6] to fracture of rubber. However, unlike rubber, which evidently fails in plane strain, giving a flat fracture, most thin sheet materials give oblique fracture planes [7], and the calculated tearing energy (per unit thickness) depends strongly on the sheet thickness.

This paper examines the thickness effect for a model polyimide material and details the nature of the deformation occurring near the crack.

## 2. Experimental technique

The polyimide studied was made by the reaction of 3,3',4,4'-benzophenonetetracarboxylic dianhydride with 4,4'-oxydianiline. Films ranging in thickness from  $\sim 7$  to  $\sim 60 \mu\text{m}$  were made from an *N,N*-dimethylacetamide solution of the amide-acid (15% solids by weight) in a dust-free, low humidity ( $< 15\%$ ) chamber. The solution was doctored on to soda-lime glass plates using various blade settings in order to achieve the different thicknesses. The cast films were dried for 24 h at room temperature in the chamber and then the glass plate and film were heated in an air oven for 1 h each at 100, 200 and 300°C. After cooling, the film was removed from the plate in a warm water bath.

Tearing energy was determined by using the "Trouser" test. Specimens ( $\sim 2.0 \text{ cm} \times \sim 15.0 \text{ cm}$ ) of each thickness were cut from the experimental films and the thicknesses were measured using a digital

micrometer; the repeatability of the thickness measurement was  $\pm 10^{-5}$  in. and the film uniformity was better than  $5 \times 10^5$  in. A tear was initiated down the centre of the specimen with a razor blade and a brass shim stock tab was glued to each "trouser leg" for gripping. With one "leg" attached to the load cell (50 g capacity) and the other to the cross-head, the specimen was then tested at a cross-head speed of  $0.08 \text{ cm min}^{-1}$ . After a critical load was reached the tear propagated down the centre of the specimen. A 1 mm wide path (marked on the specimen) served as a guideline; when the tear deviated from this path, the specimen was unloaded, the test was stopped, and the crack tip was then advanced back to the centre by hand. The load required to maintain tear propagation was determined by subtracting the load due to the specimen's weight from the load recorded during propagation. Tear forces were averaged over a distance torn of 2.5 mm or more.

For the tensile tests, specimens ( $\sim 8.0 \text{ cm} \times \sim 0.5 \text{ cm}$ ) of each thickness were cut from the experimental films using fresh razor blades. The films were then measured for their thicknesses and mounted in rubber-coated tabs creating a 5 cm gauge length. An extensometer connected to the grips was used to read out displacement, and a planimeter was used to calculate the area under the load-deflection curve. The cross-head speed was  $0.13 \text{ cm min}^{-1}$ . Deformation appeared to be uniform throughout the gauge section.

Scanning electron micrographs were obtained on fracture surfaces of tear specimens after coating with gold/palladium. Thin sections for optical microscopy were prepared by embedding torn films in epoxy resin and microtoming in a plane perpendicular to the direction of crack growth. Slices of  $\sim 5 \mu\text{m}$  thickness were examined at  $\times 200$  to  $\times 400$  using transmitted polarized light. The analyser was rotated to show the plastically deformed region most clearly.

## 3. Results and discussion

As the load-time record in Fig. 1 shows, tearing proceeded more or less continuously, but with frequent load peaks, indicating stick/slip behaviour on

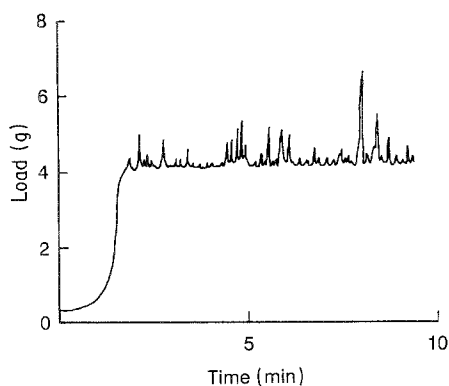


Figure 1 Typical load against time record for trousers specimen.

a fairly fine scale. A few experiments at lower and higher rates revealed that this behaviour is typical, at least over a two-decade range. In the following, the tearing force used was the average load, neglecting the sharp peaks.

An energy balance calculation [8] shows that the work per unit area torn through is given by  $2F/t_0$ , where  $F$  is the tearing force and  $t_0$  is the specimen thickness. The work per unit area of fracture surface produced is actually slightly smaller, because the fracture plane is not perpendicular to the plane of the film. Fig. 2 illustrates this "slant fracture", which was observed in all our films. It would be possible to normalize with respect to the area of the fracture plane, as Chiu and Gent did for their thicker grooved test pieces [9], but doing so is unnecessary as long as the geometry stays constant, as it does here.

Fig. 3 shows a plot of  $F/t_0$  as a function of film thickness. It is identical in form to corresponding plots

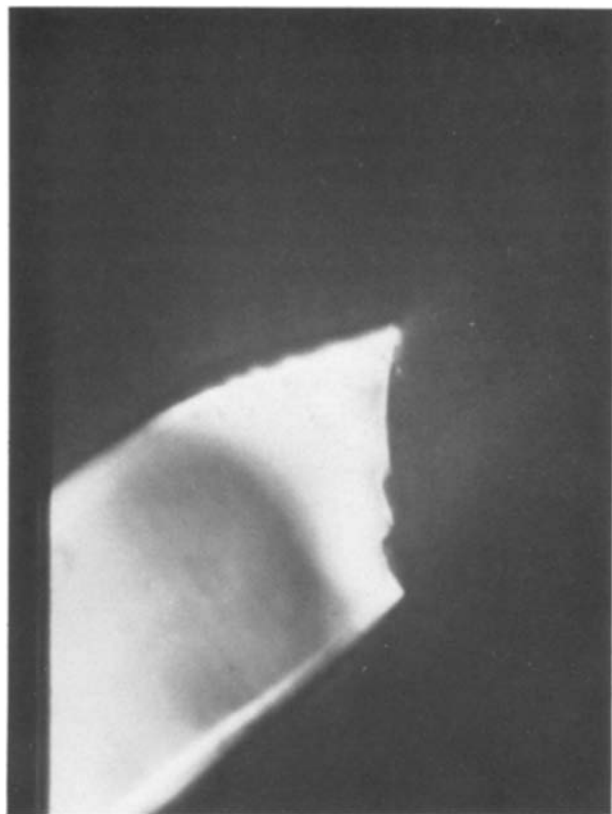


Figure 2 Microtomed section of torn specimen, viewed at  $\times 200$  between partially crossed polarizers.

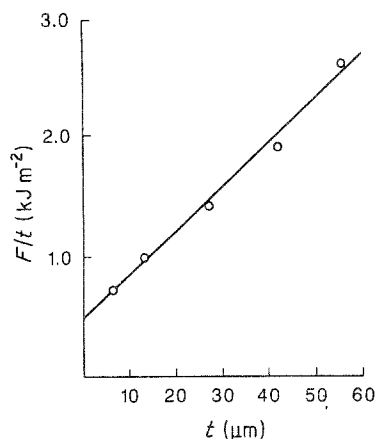


Figure 3 Normalized tearing force (tearing energy) plotted against film thickness.

for polyethylenes shown in [9]. It is significant that in a range of thicknesses often used in practical applications, neither the slope nor the intercept of Fig. 3 may be neglected. In other words, measurements at a single thickness alone could not be used to predict the tear energy at another thickness.

In order to explain the linear increase of tearing energy with film thickness, Chiu *et al.* [9] proposed a model which implicitly divides the tearing process into two parts: (1) plastic deformation in a region adjacent to the crack plane, and (2) creation of the fracture surface itself by tensile rupture. The energy associated with the latter process should depend on the area of the fracture plane, whereas the former's contribution depends on the volume of material deformed.

If we assume that the extent of the plastic zone scales with the film thickness (Fig. 4), it is then clear that the work per unit area from this source will be proportional to  $t$ , the film thickness. (It may be remarked that other models of the rupture process are possible [10]; however, for thin polymeric materials, the above description is probably realistic).

A quantitative evaluation of the model requires us to know both the volume of the plastic zone and some estimate of the strain-energy density in it. Both quantities can be arrived at objectively if certain assumptions are made. This is done below.

Plastic zone sizes can be based on analysis of cross-sectional photographs like that in Fig. 2. If the outline of Fig. 2 is reversed and redrawn, the combined profile in Fig. 5 results. In it, permanent deformation (necking) which preceded failure may be clearly seen. On this particular section, the thickness,  $t$ , of the necked-

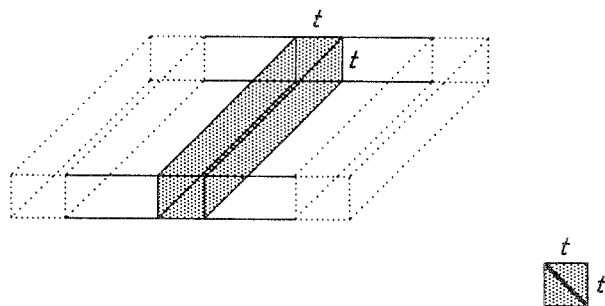


Figure 4 Model of tear specimen. Shaded region is plastic zone; inset shows cross-section perpendicular to direction of tear propagation.

TABLE I Dimensions of plastic zone

Nominal film thickness ( $\mu\text{m}$ )	Thickness reduction, $t/t_0$	Gauge length/thickness, $L_0/t_0$
14	0.801	0.91
14	0.566	0.36
25	0.704	0.79
25	0.858	0.72
25	0.833	0.76
41	0.902	0.46
41	0.946	0.72
56	0.738	0.62
56	0.826	0.67

down region is about 80% of the original film thickness,  $t_0$ . Following Kambour and Miller [11], the elongation in this region is therefore assumed to be  $t_0/t$ . (Actually this is a lower bound to the elongation, because it assumes there is no contraction in the direction of the crack). The plastically deformed region of length  $L$  in Fig. 5 had an original "gauge length" of  $L_0 = Lt/t_0$ , so we may approximate the plastic strain as occurring uniformly in a region of original dimensions  $t_0 \times L_0$ . This analysis was applied to photos of nine sections, and the results are tabulated in Table I. The apparent elongations in these sections range from ~6% to 77%, a spread which is large compared to the measurement uncertainty. However, the variations show no apparent trend with film thickness. Therefore it seems reasonable to assume that the variations are real sampling variations which occur when thin slices are excerpted from the tear path, and to average the results from all of the photos. If this is done, the plastic zone is characterized as being, on average,  $t_0$  high,  $0.67 t_0$  wide and undergoing an equivalent tensile strain of 27%.

An estimate of the strain energy in the plastic zone at rupture is obtained from the tensile stress-strain curve. For our material (Fig. 6), it is apparent that the total work to fracture in tension is almost all plastic work; Table II summarizes the tensile results. Elongations at break of individual samples ranged from 5% to 73%.

Now if the volume of material calculated earlier is used with the strain energy density from a representative tensile test, the plasticity contribution to the fracture work can be calculated to be  $20 \times 10^6 \text{ J}$

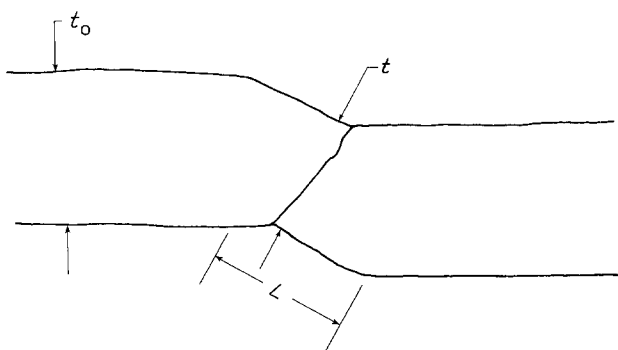


Figure 5 Reconstruction of cross-section through tear path.  $L$  is the length of the plastically deformed region.

TABLE II Tensile properties of polyimide films\*

Thickness ( $\mu\text{m}$ )	Young's modulus (GPa)	Average elongation at break (%)	Tensile strength (MPa)
58.1	3.38	10	133
47.6	3.44	39	135
26.0	3.39	36	127
12.8	3.64	12	133
6.52	3.51	7	105

\*Each value is an average from three specimens.

$\text{m}^{-3} \times t_0$ . This is significantly less than what would be implied by the slope in Fig. 3, which is  $70 \times 10^6 \text{ J m}^{-3}$ .

One factor which was not taken into account in the above analysis is the difference in rates between the tensile tests and the tear tests. In the tear tests, the effective gauge length is of the order of the film thickness, so the rate of deformation is very high — so high, in fact, that it would be impractical to try to duplicate it in a conventional tensile test. A reasonable estimate, based on the behaviour of other polymers (e.g. [12]), would be that the yield stress slightly more than doubles over the range between the rate of our tensile test and the rate of the tear. As a check on this estimate, the tearing force against log (cross-head speed) relationship can be extrapolated linearly to lower rates. Although the extrapolation is long and somewhat uncertain, this method predicts a factor of 2 to 2.5 increase in tearing force over the range considered.

Thus even if the rate effect is taken into account, the increase in tear energy with film thickness is greater than the calculated plasticity contribution. Evidently, the proposed partitioning of energy is oversimplified. In particular, it should be remembered that the tear test is a mixed-mode test (Fig. 7). Mai and Cotterell [10] have shown how in metals a shearing separation requires a work input which goes as thickness squared.

Scanning electron micrographs of the fracture surfaces of our polyimides reveal steps, plate-like structures, and roughness on a scale of tens of micrometres to a few micrometres. These structures (Fig. 8) are produced and/or distorted by the separation process, and are reminiscent of the rough appearance of Mode II and mixed-mode failures in adhesive bonds and polymer matrix composites.

#### 4. Conclusions

1. Mixed-mode tearing can be used to characterize the toughness of thin polyimide films.

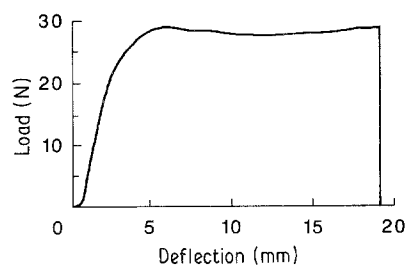


Figure 6 Tensile load-deflection curve.

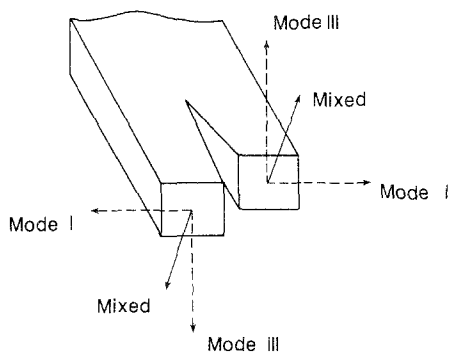


Figure 7 Schematic drawing of crack-tip region, showing deformation mode in single-tear test.

2. In the thickness range from 0 to  $55\ \mu\text{m}$ , the dependence of tearing energy on thickness is characterized by two parameters (e.g. a slope and intercept). Future work may establish the relationship of these parameters to polymer chemistry and morphology.

3. Cross-sections through the torn film indicate that the extent of deformation is highly variable. A simple comparison with deformation in tensile fracture, while instructive, does not seem to account for the details of the tearing process.

## References

1. C. E. SROOG, *J. Polym. Sci. Macromol. Rev.* **11** (1976) 161.
2. M. L. WALLACH, *J. Polym. Sci. A-2* **6** (1968) 953.
3. P. S. THEOCARIS, V. M. STARTSEV and N. F. CHUGNOVA, *Colloid Polym. Sci.* **262** (1984) 867.
4. S. A. EZZELL, A. K. St. CLAIR and J. A. HINKLEY, *Polymer* in press.
5. ASTM D1938-67, Annual Book of ASTM Standards (American Society for Testing and Materials, Philadelphia, 1986).
6. R. S. RIVLIN and A. G. THOMAS, *J. Polym. Sci.* **10** (1953) 291.
7. D. P. ISHERWOOD and J. G. WILLIAMS, *Engng Fract. Mech.* **10** (1978) 887.
8. G. E. ANDERTON and L. R. G. TRELOAR, *J. Mater. Sci.* **6** (1971) 562.
9. D. S. CHIU, A. N. GENT and J. R. WHITE, *ibid.* **19** (1984) 2622.
10. Y. W. MAI and B. COTTERELL, *Int. J. Fract.* **24** (1984) 229.
11. R. KAMBOUR and S. MILLER, *J. Mater. Sci.* **11** (1976) 823.
12. R. A. DUCKETT, S. RABINOWITZ and I. M. WARD, *J. Mater. Sci.* **5** (1970) 909.

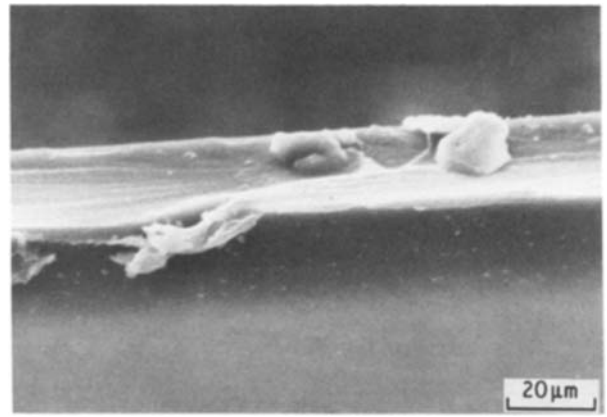


Figure 8 Scanning electron micrograph of fracture surface of tear specimen.

Received 16 February  
and accepted 29 April 1987